A mathematical model of β-cells in an islet of Langerhans sensing a glucose gradient

Michael Meyer-Hermann[1] and Richard K. P. Benninger[2]

[1]Frankfurt Institute for Advanced Studies (FIAS), Ruth-Moufang-Strasse 1, 60438 Frankfurt/Main, Germany
[2]Molecular Physiology and Biophysics, 74OA Light Hall, Vanderbilt University, Nashville, Tennessee 37232, USA

(Received 14 December 2009; accepted 10 February 2010; published online 8 April 2010)

Pancreatic β-cells release insulin in response to increased glucose levels. Compared to isolated β-cells, β-cells embedded within the islets of Langerhans network exhibit a coordinated and greater insulin secretion response to glucose. This coordinated activity is considered to rely on gap-junctions. We investigated the β-cell electrophysiology and the calcium dynamics in islets in response to glucose gradients. While at constant glucose the network of β-cells fires in a correlated fashion, a glucose gradient induces a sharp division into an active and an inactive part. We hypothesized that this sharp transition is mediated by the specific properties of the gap-junctions. We used a mathematical model of the β-cell electrophysiology in islets to discuss possible origins of this sharp transition in electrical activity. In silico, gap-junctions were required for such a transition. However, the small width of transition was only found when a stochastic variability of the expression of key transmembrane proteins, such as the ATP-dependent potassium channel, was included. The agreement with experimental data was further improved by assuming a delay of gap-junction currents, which points to a role of spatial constraints in the β-cell. This result clearly demonstrates the power of mathematical modeling in disentangling causal relationships in complex systems. [DOI: 10.2976/1.3354862]

CORRESPONDENCE
Michael Meyer-Hermann:
m.meyer-hermann@
fias.uni-frankfurt.de

The electrophysiology of β-cells is most relevant for understanding insulin secretion (Rorsman and Renstrom, 2003). Exocytosis of insulin loaded granules is dependent on intracellular calcium signaling. Glucose transport and metabolism induces the synthesis of adenosine triphosphate (ATP) in the mitochondria of β-cells. This increases the cellular ATP to adenosine diphosphate (ADP) ratio and inhibits ATP-sensitive potassium (K-ATP) channels. The reduced outflow of potassium depolarizes the β-cell and opens voltage-dependent calcium channels. Oscillations between calcium inwards and potassium outwards currents are induced leading to bursts of the membrane potential. A slow increase in the intracellular calcium is triggered that at some level interrupts the oscillation. The increased calcium level is at the same time the triggering event for an increased exocytosis frequency of insulin carrying granules (Gilon *et al.*, 2002).

In experiments, a prominent difference in the stability of bursts in excitable β-cells was observed depending on whether the β-cells are isolated or in their natural environment within the islet of Langerhans (Zhang *et al.*, 2003). While isolated β-cells exhibit unstable bursting, β-cells in an islet context show strongly correlated activity. This stability is attributed to the connection of β-cells with gap-junctions (Ravier *et al.*, 2005; Rocheleau *et al.*, 2006). However, the detailed role of gap-junctions for β-cell electrophysiology and calcium dynamics is not well understood and a matter of debate.

We are convinced that a mathematical model of β-cells coupled by gap-junctions will help to disentangle their impact on β-cell electrical activity in islets. So far, two β-cells have

been coupled by gap-junction (Jo *et al.*, 2005) based on a model of the β-cell electrophysiology (Sherman *et al.*, 1988; Sherman, 1996). These are based on a subset of transmembrane currents and well reproduce the behavior of β-cells. A possible role of noise was considered to induce stabilization of electrical bursting (de Vries and Sherman, 2000; Jo *et al.*, 2005). Bigger maps of coupled cells were considered in view of bursting (de Vries, 2001) and more recently with particular emphasis on pancreatic β-cells (Giugliano *et al.*, 2000; Benninger *et al.*, 2008).

A previously developed quantitative model of the β-cell electrophysiology (Meyer-Hermann, 2007) is fully based on measured single transmembrane properties and is, thus, considered as a good starting point for a map of coupled β-cells. Here, this model was combined with the gap-junction model in (Benninger *et al.*, 2008) using β-cells arranged in a regular grid with defined neighborhood relations. The electrical activity throughout the modeled islet was considered for different applied glucose levels and for stable glucose gradients along the islet.

The modeling results were compared to experimental results (Rocheleau *et al.*, 2004). It was found *in silico* that the gap-junctions induce a correlation of β-cell activity in the islet. The stability of the correlation can be perturbed with stochastic variations in some quantities (as found before in (Jo *et al.*, 2005). A delay of the adaptation of the gap-junction current to changed intracellular properties turns out to induce nonlinear (chaotic) effects in the islet. When applying a glucose gradient along the islet a sharp division of the islet into an active and an inactive part is found in the experiment. This transition could be reproduced in the model by assuming a stochastic variation in K-ATP channel expression levels.

RESULTS

The goal of this work was to develop a mathematical model of the β-cell electrophysiology that allows an analysis of the impact of gap-junctions between β-cells coupled in islets of Langerhans on electrical activity and calcium dynamics. The resulting mathematical model and the analysis of gap-junctions under different conditions are presented. In particular, we applied different levels of glucose to the whole islet as well as glucose gradients along the islet.

Model development

We investigated the activity of β-cells in an islet that are connected by gap-junctions. A two-dimensional network of 27 β-cells arranged in a block of 3×9 cells was used. Each β-cell is assumed to exhibit exactly the same properties as in the model for isolated cells (Meyer-Hermann, 2007). The extension of this model to gap-junction coupling is described as follows.

Rate equations are used to describe the dynamics of intracellular ion concentrations. External ion concentrations are treated as a thermodynamic bath and are assumed to be constant. The ions treated explicitly are sodium (N), potassium (K), and calcium (C). The dynamics depend on the conductance of various membrane proteins, where each corresponds to a single term in the following differential equations.

$$\frac{dN}{dt} = -\frac{\xi}{F}\left(\rho_{\mathrm{Na,V}} I_{\mathrm{Na,V}} + 2\rho_{\mathrm{Na,K}} I_{\mathrm{Na,K}} \alpha_{\mathrm{Na,K}} + \rho_{\mathrm{NCX}} I_{\mathrm{NCX}} \alpha_{\mathrm{NCX}} + \frac{1}{6}\sum_{j=1}^{n} \rho_{\mathrm{gap}} I^{\mathrm{Na}}_{\mathrm{gap},j} + J_{\mathrm{Na}}\right)$$

$$\frac{dK}{dt} = -\frac{\xi}{F}\left(\rho_{\mathrm{K,ATP}} I_{\mathrm{K,ATP}} + \rho_{\mathrm{K,V}} I_{\mathrm{K,V}} + \rho_{\mathrm{sK,Ca}} I_{\mathrm{sK,Ca}} + \rho_{\mathrm{K,Ca}} I_{\mathrm{K,Ca}} - 2\rho_{\mathrm{Na,K}} I_{\mathrm{Na,K}} + \frac{1}{6}\sum_{j=1}^{n} \rho_{\mathrm{gap}} I^{\mathrm{K}}_{\mathrm{gap},j} + J_{\mathrm{K}}\right)$$

$$\frac{dC}{dt} = -\frac{\xi}{z_{\mathrm{Ca}} F(1+x_b)}\left(\rho_{\mathrm{Ca,L}} I_{\mathrm{Ca,L}} + \rho_{\mathrm{Ca,T}} I_{\mathrm{Ca,T}} - z_{\mathrm{Ca}}\rho_{\mathrm{NCX}} I_{\mathrm{NCX}} + \rho_{\mathrm{PMCA}} I_{\mathrm{PMCA}} + \frac{1}{6}\sum_{j=1}^{n} \rho_{\mathrm{gap}} I^{\mathrm{Ca}}_{\mathrm{gap},j} + J_{\mathrm{Ca}}\right). \quad (1)$$

Here, I_x denote the membrane currents, where x specifies the type of membrane protein, which are listed in Table I. Negative currents are defined to bring positive ions into the cell. The I_x are defined as single channel/protein conductance and corresponding currents can be derived from experiments

Table I. Acronyms for the different plasma membrane proteins contributing to ion flow through the membrane. *Inwards* and *outwards* specifies in which direction the ion flows, i.e., in or out of the cell.

Na,K	Sodium-potassium exchanger (Na^+ outwards, K^+ inwards)
Na,V	Voltage-gated sodium channels (inwards)
NCX	Sodium-calcium exchanger (Na^+ inwards, Ca^{2+} outwards)
PMCA	ATP-driven plasma-membrane-calcium-ATPase (Ca^{2+} outwards)
K,ATP	ATP-driven (and glucose-dependent) potassium channels (outwards)
K,V	Voltage-gated potassium channels (delayed rectifier) (outwards)
sK,Ca	Small conductance calcium-gated potassium channel (outwards)
K,Ca	Large conductance voltage- and calcium-gated potassium channel (outwards)
Ca,L	L-type voltage-dependent calcium channels (inwards)
Ca,T	T-type voltage-dependent calcium channels (inwards)
Gap	Gap-junction conducting all ions

[see Meyer-Hermann (2007)]. n in the term for the gap-junction stands for the number of connected neighbor cells. ρ_x denote the corresponding surface densities of the membrane proteins. ξ is the surface to volume factor that translates the transmembrane current into a space-averaged intracellular change in the ion concentration. The factors $\alpha_{\mathrm{NCX,Na,K}}$ account for the stoichiometry of exchangers. $z_{\mathrm{Ca}}=2$ is the valence of calcium ions. The leakage currents $J_{\mathrm{K,Na,Ca}}$ are defined to guarantee a stable resting state of the cell. In the resting state all other currents are balanced by the leakage currents.

Calmodulin is a calcium buffer. It is assumed to bind calcium faster than the typical time scale of the ion dynamics and the membrane potential. Thus, we use the rapid buffer approximation. This gives rise to the additional factor $(1+x_b)$ in the equation for calcium Eq. (1).

$$x_b = \frac{b_0 K_b}{(\mathrm{C}+K_b)^2}, \tag{2}$$

where b_0 is the total buffer concentration and K_b is the corresponding dissociation constant.

The dynamics of these ions build up the membrane potential V.

$$\begin{aligned}\frac{dV}{dt} = -\frac{1}{C_m}\Bigg(&\rho_{\mathrm{Na,K}} I_{\mathrm{Na,K}} + \rho_{\mathrm{K,ATP}} I_{\mathrm{K,ATP}} + \rho_{\mathrm{K,V}} I_{\mathrm{K,V}} \\ &+ \rho_{\mathrm{sK,Ca}} I_{\mathrm{sK,Ca}} + \rho_{\mathrm{K,Ca}} I_{\mathrm{K,Ca}} + \rho_{\mathrm{Na,V}} I_{\mathrm{Na,V}} + \rho_{\mathrm{NCX}} I_{\mathrm{NCX}} \\ &+ \rho_{\mathrm{PMCA}} I_{\mathrm{PMCA}} + \rho_{\mathrm{Ca,L}} I_{\mathrm{Ca,L}} + \rho_{\mathrm{Ca,T}} I_{\mathrm{Ca,T}} \\ &+ \sum_x \frac{1}{6}\sum_{j=1}^{n} \rho_{\mathrm{gap}} I^x_{\mathrm{gap},j} + J_{\mathrm{K}} + J_{\mathrm{Na}} + J_{\mathrm{Ca}}\Bigg).\end{aligned} \tag{3}$$

where the same terms as in Eq. (1) appear. Note that all currents are defined to be electrical currents. Thus, the contributions enter without additional factor in Eq. (3) but have additional factors in Eq. (1) in the case that a single electrical charge does not correspond to a single ion passing the membrane. C_m is the membrane capacitance and replaces the surface to volume ratio ξ used in the case of ion concentrations. Typical values are $C_m=0.01$ pF/μm^2 (Chay, 1997) or 0.0009 pF/μm^2 [for neurons, Gentet *et al.* (2000)].

All currents $I_{XX,YY}$ (where the subscript is one of the acronyms in Table I) are derived from single transmembrane protein characteristics. This is described in detail in (Meyer-Hermann, 2007). In the following the additional gap-junction current is specified.

Model of gap-junction currents: The term entering all ionic differential equations of cell i and which was previously used in (Benninger *et al.*, 2008) is in more general terms

$$\sum_{j=1}^{n} \frac{1}{6}\rho_{\mathrm{gap},ij} I^{\mathrm{ion}}_{\mathrm{gap},ij}, \tag{4}$$

where the sum goes over all n connected neighbors j and the currents are different for different ions. Assuming the density of gap-junctions to be identical for all cell-cell connections we have $\rho_{\mathrm{gap},ij} \equiv \rho_{\mathrm{gap}}$.

β-cells are connected with the gap-junction protein connexin-36 (Moreno *et al.*, 2004). The whole cell conductance mediated by these junctions is in the order of 500–1,000 pS (Zhang *et al.*, 2008). A single gap-junction has a conductance of 5.1±0.7 pS (Moreno *et al.*, 2004). One cell-cell connection is assumed to be concentrated within 1/6 of the cell surface. Assuming 30 gap-junctions per contact infers

$$\frac{1}{6} 4\pi R^2_{\mathrm{cell}} \rho_{\mathrm{gap}} = 30 \Rightarrow \rho_{\mathrm{gap}} = \frac{180}{4\pi R^2_{\mathrm{cell}}}. \tag{5}$$

Indeed, then for six neighbors we have

$$4\pi R^2_{\mathrm{cell}} \sum_{j=1}^{6} \frac{1}{6} \rho_{\mathrm{gap}} \overline{g_{\mathrm{gap}}} = \sum_{j=1}^{n} 30 \overline{g_{\mathrm{gap}}} \tag{6}$$

$$= 180 \overline{g_{\mathrm{gap}}} \sim 918 \ \mathrm{pS} \tag{7}$$

using the physiological single gap-junction conductance of 5.1 pS, which is in agreement with the value 950±96 pS (Zhang *et al.*, 2008).

Note that if a cell has only three, four, or five neighbors (such at the border) the resulting total conductance is reduced according to the real number of neighbors. This assumes that the connections between two cells are always of the same type. In 2D-simulations, the density is still calculated according to a 3D-cell with six connections because the density is related to the surface of the 3D-cell. However, in 2D the maximum number of connections is $2D=4$ and the total possible gap-current is, thus, reduced by a factor of 2/3 (see the factor 1/6 in Eq. (4), which in principle, could also be replaced by $1/(2D)$ in a different strategy with D the dimension of the simulation space).

Connexin-36 has a very weak voltage gating (Moreno *et al.*, 2004) so that a constant conductance can be safely assumed. The channels between β-cells are much bigger than the ions, and allow molecules of up to 1 kDa or 2 kDa to pass. Nevertheless, the resulting current depends on the potential difference in both connected cells and the ion-specific reversal potential.

$$I^x_{\mathrm{gap},ij} = \overline{g_{\mathrm{gap}}} V^x_{\mathrm{gap},ij} \tag{8}$$

with

$$\frac{dV^x_{\mathrm{gap},ij}}{dt} = \frac{\overline{V^x_{\mathrm{gap},ij}} - V^x_{\mathrm{gap},ij}}{\tau^x_{\mathrm{gap}}} \tag{9}$$

The asymptotic potential difference is

$$\overline{V^x_{\mathrm{gap},ij}} = (V_i - V_j - \tilde{V}^x_{ij}) \tag{10}$$

with the latter term representing the Nernst-potential

$$\tilde{V}^x_{ij} = \frac{RT}{z_x F} \ln\left(\frac{x_j}{x_i}\right). \tag{11}$$

$x = \mathrm{K}, \mathrm{Na}, \mathrm{Ca}$ and $R = 8.315\ \mathrm{J/(K\ mol)}$ is the Rydberg (molar) gas constant. The temperature T has to be adopted to the experimental situation or the *in vivo* case. $x_{i,j}$ are the intracellular ionic concentrations of the cells i and j, respectively. Note that the currents are symmetric by construction, i.e.,

$$I^x_{\mathrm{gap},ji} = -I^x_{\mathrm{gap},ij}. \tag{12}$$

In this approach it is assumed that the point of ionic currents between the extracellular medium and the cytosol is separated from the location of the gap-junction, such that changes in the ionic intracellular concentrations become effective on the level of the gap-junction with a time delay τ^x_{gap}. The delay can be estimated from the diffusion constant and the distance that has to be overcome together with typical diffusion constants. The distance is assumed to be in the order of the cell radius around 6 μm. The diffusion constant is in the range of 223 $\mu\mathrm{m}^2/\mathrm{s}$ (Allbritton *et al.*, 1992). This gives rise to

$$\tau^x_{\mathrm{gap}} \sim \frac{\Delta x^2}{D_x} \approx \frac{36\ \mu\mathrm{m}^2}{223\ \mu\mathrm{m}^2/\mathrm{s}} = 161\ \mathrm{ms}, \tag{13}$$

where the diffusion constant was simply assumed equal for all ions. One might argue whether the delay also applies to the membrane potential $V_i - V_j$ or to the Nernst-term only. One might also argue that the gap-junctions themselves give rise to a delay in activity, which would be in analogy to other transmembrane proteins. In addition, on the scale of 161 ms the local changes in ions are already equilibrated in the sense that sodium and potassium exchange is achieved on the scale of milliseconds. Thus, a big part of the concentration changes might never reach the gap-junctions. Taken together these thoughts make the exact value of the delay rather uncertain and we, therefore, also evaluated delays in the range of a few to 500 ms in the simulations.

In the resting state $V_i = V_j$ and $x_i = x_j$ holds, implying a vanishing Nernst-potential and gap-junction current. This also implies that the leakage currents, which are determined to guarantee the resting state of the cells, are not altered by gap-junctions.

In the limit $\tau \to 0s$ the current equation for gap-junctions simplifies to

$$I^x_{\mathrm{gap},ij} = \overline{g_{\mathrm{gap}}}(V_i - V_j - \tilde{V}_x). \tag{14}$$

β-cell synchronization in islets at constant glucose

The glucose level is set to 10 mM throughout the islet. The cell activity in this *in silico* islet with β-cells connected by gap-junctions turns out to be correlated and fully synchronized. The synchronous behavior of all β-cells is the same as the one published for an isolated *in silico* β-cell at 10 mM stimulation (see Meyer-Hermann (2007); data not shown). The synchronization is well supported by experiment, where more than 90% of electrically active cells in an islet oscillated synchronously (Benninger *et al.*, 2008).

Connected β-cells in an islet with glucose gradient

Next the glucose concentration was varied from 2 mM to 12 mM at both ends of the long direction of the modeled islet. In experiment synchronous calcium oscillations are seen in the side of the islet stimulated with 12 mM glucose. There is a sharp transition of less than two cells width, where oscillations are halted. The oscillations in calcium are halted at a point in the islet that is stimulated with an average of 7.2 ± 0.6 mM glucose, determined by NAD(P)H imaging (Rocheleau *et al.*, 2004).

We asked whether and under which conditions this transition between an active and an inactive part of the islet is found *in silico*. Applying the same glucose gradient, the β-cells exhibited a degree of excitation that continuously followed the glucose level (Fig. 1 right panel). Thus, the sharp transition found in experiment was not reproduced. There are three striking observations: first, bursting at 10 mM glucose is not comparable to isolated *in silico* cells at 10 mM glucose. The β-cells at high glucose exhibit a pronounced spike instead of a burst (Fig. 1 left panel). Second, β-cells exhibit a remaining activity at glucose levels, where isolated *in silico* cells do not spike at all (Fig. 1 left panel, blue and green curve). Third, the activity of the β-cells is correlated throughout the islet, i.e., all cells fire in phase (Fig. 1).

Mimicking space with a delayed gap-junction current

A role of noise was postulated to impact on β-cells in islets (de Vries and Sherman, 2000; Jo *et al.*, 2005). We asked whether it is possible to get desychronized firing of coupled β-cells and the observed transition in a glucose gradient with a deterministic model. The used model for the β-cell electrophysiology (Meyer-Hermann, 2007) does not resolve the intracellular space. However, the position of calcium entry points in the plasma membrane and the gap-junctions are not necessarily the same. The locally increased calcium level might need to diffuse to the gap-junction. The distance between both channels will induce a delay of the gap-junction current with respect to the time of calcium entry. Also, the quick clearance of calcium will reduce the calcium concentration that reaches the gap-junction.

A proper model for these effects would be based on a model that resolves the intracellular space and includes intracellular organelles. We leave this for future investigations and estimated here, whether these effects might change the behavior of connected β-cells. To this end, a phenomeneological time delay of the current adaptation at the gap-

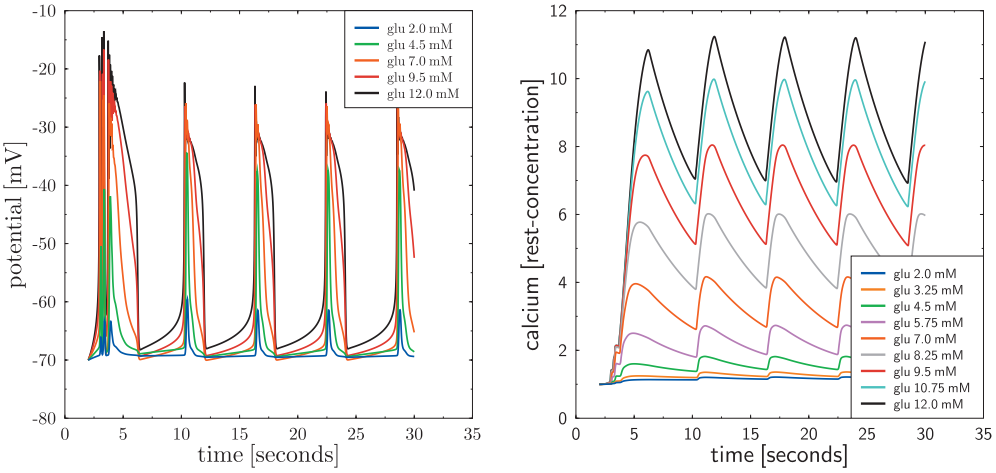

Figure 1. β-cell activity and calcium levels in an islet. 27 β-cells are arranged in 2D in three rows of length of nine cells. The β-cells are connected with gap-junctions (30 junctions per cell-cell contact with 5.1 pS conductance each). The islet is stimulated with a linear glucose gradient of 2–12 mM in the direction of the nine cells. It is found that the β-cells do not burst (left panel) and that calcium continuously follow the glucose level (right panel).

junction to the space-averaged ion concentrations of the cell is used [see Eq. (9)]. The delay was estimated by the typical size of a β-cell to be given by Eq. (13). In contrast to the *in silico* islet without delay of gap-junctions, now bursting of all β-cells in the islet is induced (Fig. 2 upper left panel). The burst are correlated throughout the islet (see Fig. 2 upper left panel). The overall level of reached calcium is reduced (see Fig. 2 upper right panel). However, the transition between an active and an inactive part of the islet with a glucose gradient is not altered, in particular, it did not become sharper (Fig. 2 upper right panel).

Unstable behavior for long delays of the gap-junction current

When increasing the delay to 500 ms, the β-cell activity is only weakly correlated (Fig. 2 lower panels). The nonlinearity of the model becomes a visible property of the model. The transition between an active and an inactive part of the islet is now more pronounced even though not reaching the desired sharp transition. [See also Supplementary Material Movie; the movie shows 3×9 β-cells in a two-dimensional plane connected by gap-junctions. Each cell-cell connection contains 30 gap-junctions with a conductance of 5.1 pS each. The gap-junction currents adapt to the cytosolic state of the cell with a delay of 500 ms. The color codes the membrane potential from low (blue) to high (red).] Note that the activity of β-cells is interrupted in the whole islet with irregular intervals (Fig. 2 lower left panel)

The membrane potentials of individual cells in an islet with glucose gradient are shown in Fig. 3 for a delay of 50 ms (upper panels) and 500 ms (lower panels). It can be seen that the longer delay induces less activity in the membrane potential for the same glucose level. This confirms that the transition between an active and inactive part of the islet is sharper for longer gap-junction delays.

Synchronization of β-cells by strong gap-junction coupling

How is the islet behaving when the gap-junction current is increased? It is expected that strong gap-junction currents will induce a stronger coupling of all β-cells in the islet. Indeed, a 25-fold gap-junction current induces a stronger correlation of β-cell spiking and almost identical calcium waves among all connected β-cells (see Fig. 4). No bursts but single spikes are observed. Interestingly, also, the β-cells that see a glucose level of only 2 mM now spike and exhibit calcium waves. Thus, gap-junctions can induce synchronization of islet β-cells down into the part of the islet that senses glucose levels below the β-cell activity threshold.

Gap-junction knock-out

In a gap-junction knock-out experiment, the gap-junction density is set to zero for all β-cells in the islet. This electrically isolates all β-cells and allows us to consider their behavior as isolated cells for different glucose levels. The corresponding spiking or bursting behavior is depicted in Fig. 5. This might be compared to an islet sensing the same glucose gradient but with β-cells connected by gap-junctions in Fig. 3 (using a 50 ms delayed gap-junction current). It can be seen that connected β-cells exhibit activity at glucose levels for which the isolated β-cells in this knock-out experiment do not show any activity. This, demonstrates that gap-junctions have the capability to transport the activity of β-cells to regions of the islet at which subcritical glucose levels are encountered. This confirms the relevance of gap-junctions for the activity of β-cells embedded in islets.

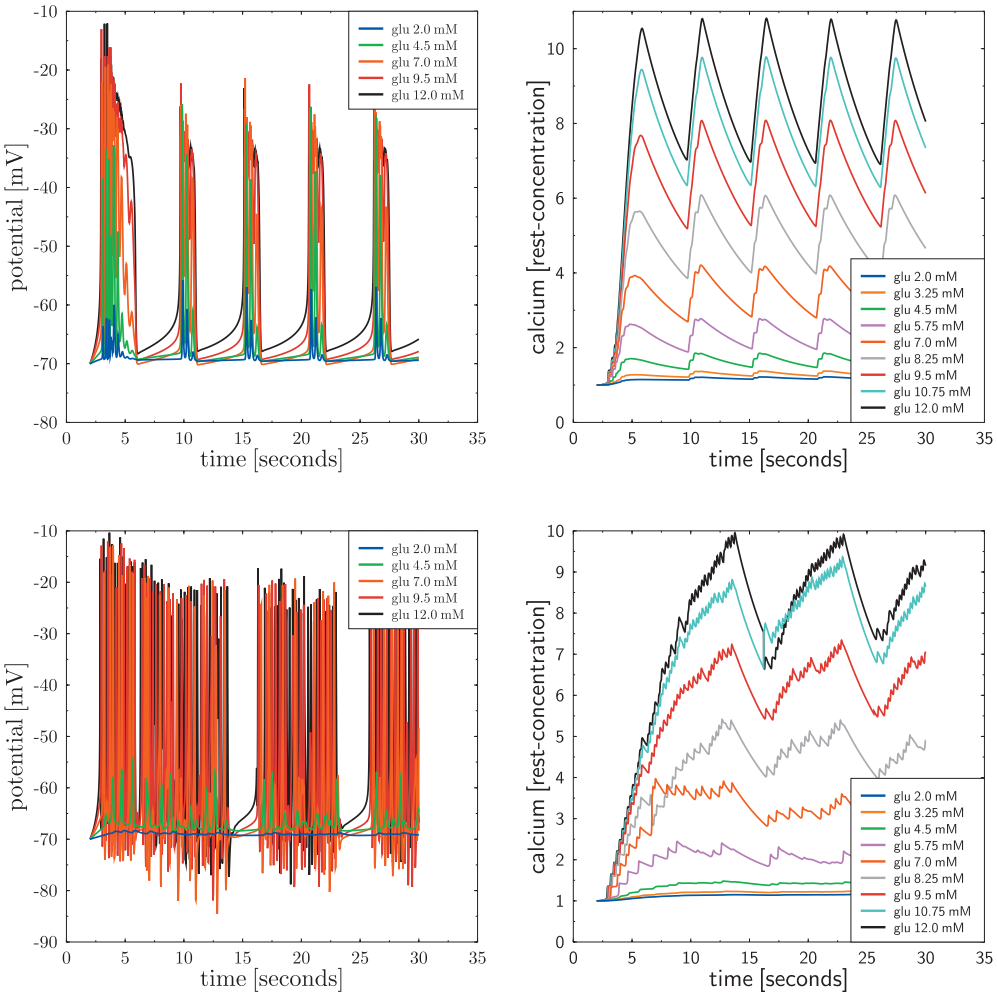

Figure 2. β-cell activity and calcium levels in an islet with delayed gap-junctions. 27 β-cells are arranged in 2D in three rows of length of nine cells. The β-cells are connected with gap-junctions (30 junctions per cell-cell contact with 5.1 pS conductance each). Gap-junction currents are delayed by 18 ms (upper panels) and 500 ms (lower panels). The islet is stimulated with a linear glucose gradient of 2–12 mM in the direction of the nine cells. Correlated bursts throughout the islet are found. For a long delay of 500 ms the electrical activity exhibit signs of unstable behavior.

No major effect of a random variation in gap-junction strength

The gap-junction density, so far, was assumed to be identical for all β-cell connections in the islet. We asked about the impact of individual gap-junction densities for different connections. The random choice of the individual gap-junction expression level was done in a simple way.

$$\rho_{\mathrm{gap},ij} = \rho_{\mathrm{gap}}(1 + r - a). \tag{15}$$

For all neighbor pairs ij, where $r \in [0, 2a]$ is a random number and a determines the range of variability, which is set to $a = 0.5$ here. In average the expression level is identical to the value ρ_{gap} that was previously used for all β-cells.

Using this range of expression levels between 50% and 150% noise is introduced to the system but the general behavior of the system does not change (data not shown). Thus, a stochastic variation in gap-junction currents does not induce major effects onto β-cell activity in islets.

Stochastic K-ATP expression with a glucose gradient on the islet

In order to get a sharper transition between the active and the inactive part of the islet, we investigated a stochastic expression of K-ATP-channels. The random expression level of the K-ATP-density is chosen according to the law in Eq. (15) with $a = 0.5$. At spatially constant glucose levels of 10 mM this variation exhibited division of the islet into two distinguished groups of cells. The two groups differed in the degree of calcium activity (see Fig. 6 upper panels).

This observation depends on the random number generator seed value and the grouping can be more or less pronounced compared to the example shown in Fig. 6. In particular, the depicted example exhibits high calcium activity

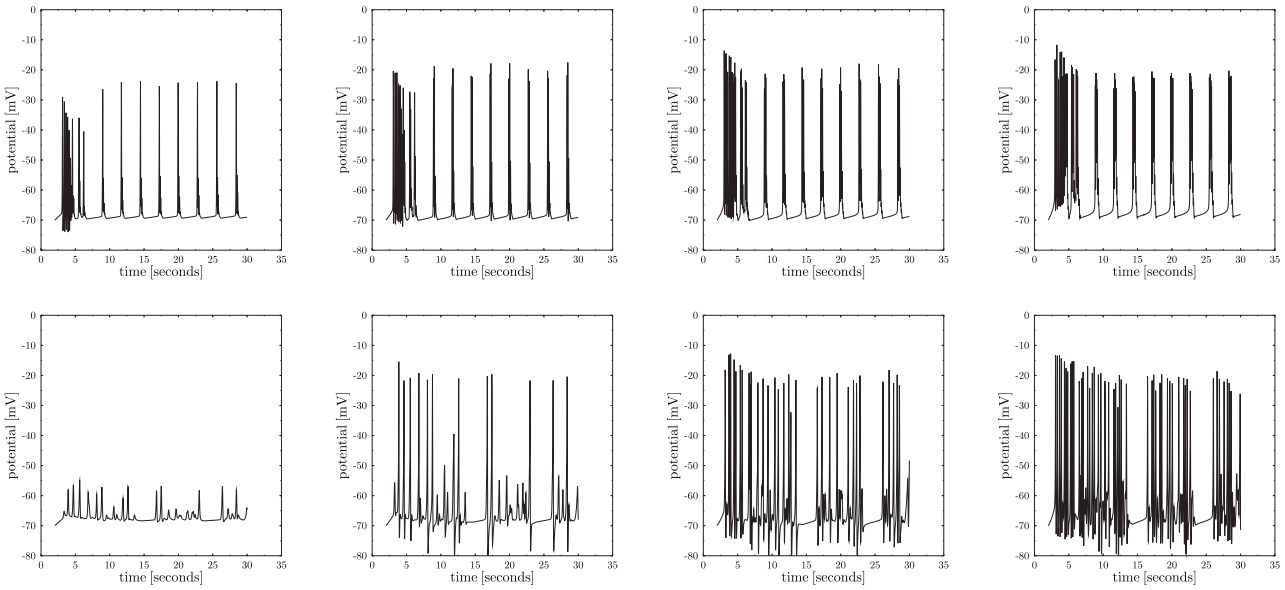

Figure 3. β-cell membrane potential of single cells in an islet with glucose gradient. The glucose levels are 4.5 mM, 5.75 mM, 7.0 mM, and 8.25 mM, respectively, for the panels from left to right. The assumed delay of gap-junction adaptation is 50 ms (upper panels) and 500 ms (lower panels).

in the part of the islet that corresponds to the low glucose part in the case of application of a glucose gradient. Thus, a division of the islet into an active and inactive part could not be expected or might even be suppressed for this random number seed. Surprisingly, this is not the case. Even though the grouping is not very pronounced it is still stronger than without K-ATP stochasticity (data not shown).

Using a different random number generator seed value that does not induce a strong grouping at constant glucose, no bias is set by the random K-ATP-expression profile. Then, the activity division of the islet into two parts became even more pronounced (see Fig. 6 lower panels). As in experiment (Rocheleau *et al.*, 2004), the transition from the active to the inactive part happens within a width of two cells at glucose levels between 5.75 mM and 7.0 mM. The classification is more pronounced for a longer time delay of gap-junction adaptation (compare Fig. 6, right panels).

Within the active part of the islet the β-cells now exhibit the behavior expected from experiment (see Fig. 6 lower panels).

- The calcium amplitude became similar for all active β-cells.

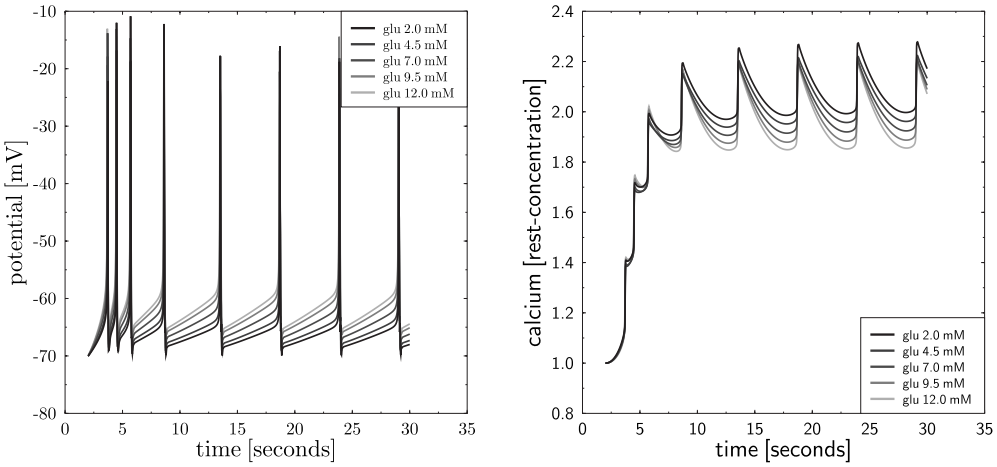

Figure 4. β-cell activity and calcium levels in a highly connected islet. 27 β-cells are arranged in 2D in three rows of length of nine cells. The β-cells are connected with gap-junctions (200 junctions per cell-cell contact with 20 pS conductance each). Gap-junction currents are delayed by 50 ms. The islet is stimulated with a linear glucose gradient of 2–12 mM in the direction of the nine cells. β-cells are fully correlated and exhibit single spiking. Calcium oscillations are nearly on the same level.

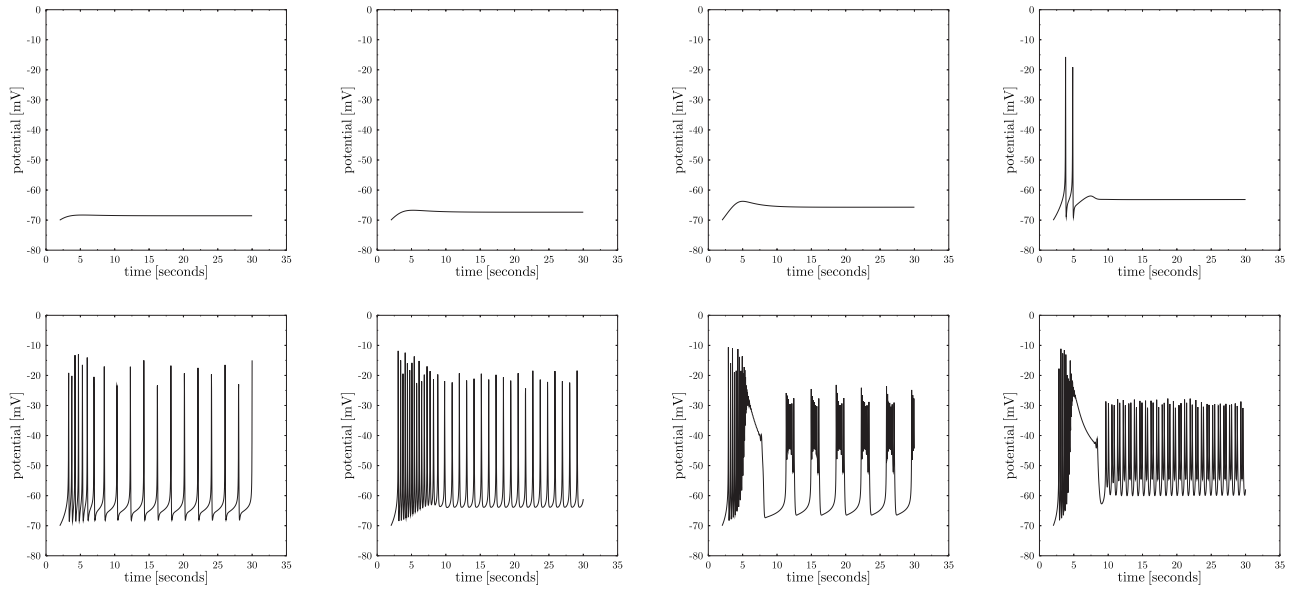

Figure 5. β-cell membrane potential of isolated cells in an islet with glucose gradient. β-cells are not connected by gap-junctions. The glucose levels are 3.25 mM, 4.5 mM, 5.75 mM, 7.0 mM, 8.25 mM, 9.5 mM, 10.75 mM, and 12.0 mM, respectively, for the panels in reading order.

- The absolute calcium level scales weakly with the glucose gradient.
- The activity of all β-cells in the active part of the islet is synchronized.

The inactive β-cells show a remaining low activity, which is not reflected in the membrane potential by bursts but by single spikes. This is shown for the two β-cells representing the transition from the active to the inactive part in Fig. 6 (lower right panel) at 5.75 mM and 7.0 mM glucose (see Fig. 7).

DISCUSSION

We have investigated β-cell coupling in islets based on experimental data (Rocheleau *et al.*, 2004) by combining a quantitative mathematical model of β-cell electrophysiology (Meyer-Hermann, 2007) with a recent mathematical model for gap-junctions (Benninger *et al.*, 2008). The interesting experimental observation of the division of islets into an active and an inactive part after application of a glucose gradient was analyzed. Experiments show a balance in the coupling mechanisms sufficient to synchronize stimulated region but not enough to allow propagations into unstimulated region. This result is reproduced by the newly developed model for β-cell electrophysiology including gap-junctions. It is found *in silico* that coupled β-cells fire in a synchronous way throughout the islet if a spatially constant glucose level is applied. A glucose gradient induces a graded behavior of coupled β-cells. A division of the islet into an active and an inactive part of the islet is not observed and only slightly promoted by a delay of gap-junction adaptation to changed intracellular membrane potential and ion concentrations.

Previous theoretical work for different cells (de Vries, 2001) and for single β-cells (Jo *et al.*, 2005) suggest a role of stochastic expression levels on β-cell coupling. This was further supported by the observation that the number of gap-junctions per cell-cell connection varies by at least 50%. In the present model stochastic variation in the gap-junction expression level did not exhibit a strong effect on the transition between active and inactive parts of the islet in a glucose gradient.

Thus, the mathematical model can only qualitatively describe the behavior found in experiment. The model of coupled β-cells confirms a role of gap-junctions in coordinating electrical activity. As the agreement between theory and experiment was not fully quantitative we used the model to find hints for an explanation of the sharp transition between the active and inactive parts of islets in a glucose gradient. One might consider to add missing currents, or that the way we handle the coupling architecture or mechanism of action is not fully correct. A $\sim$20% decrease in gap-junction conductance was observed at 2 mM compared to 11 mM (unpublished data). Also, a weak voltage gating of the gap-junction (Moreno *et al.*, 2004) may impact on the results.

The most important hint coming from the present model is the reproduction of the experimentally observed sharp transition from active to inactive β-cells in response to stochastic variation in the expression levels of K-ATP channels. A 50% variation leads to a transition with characteristics that

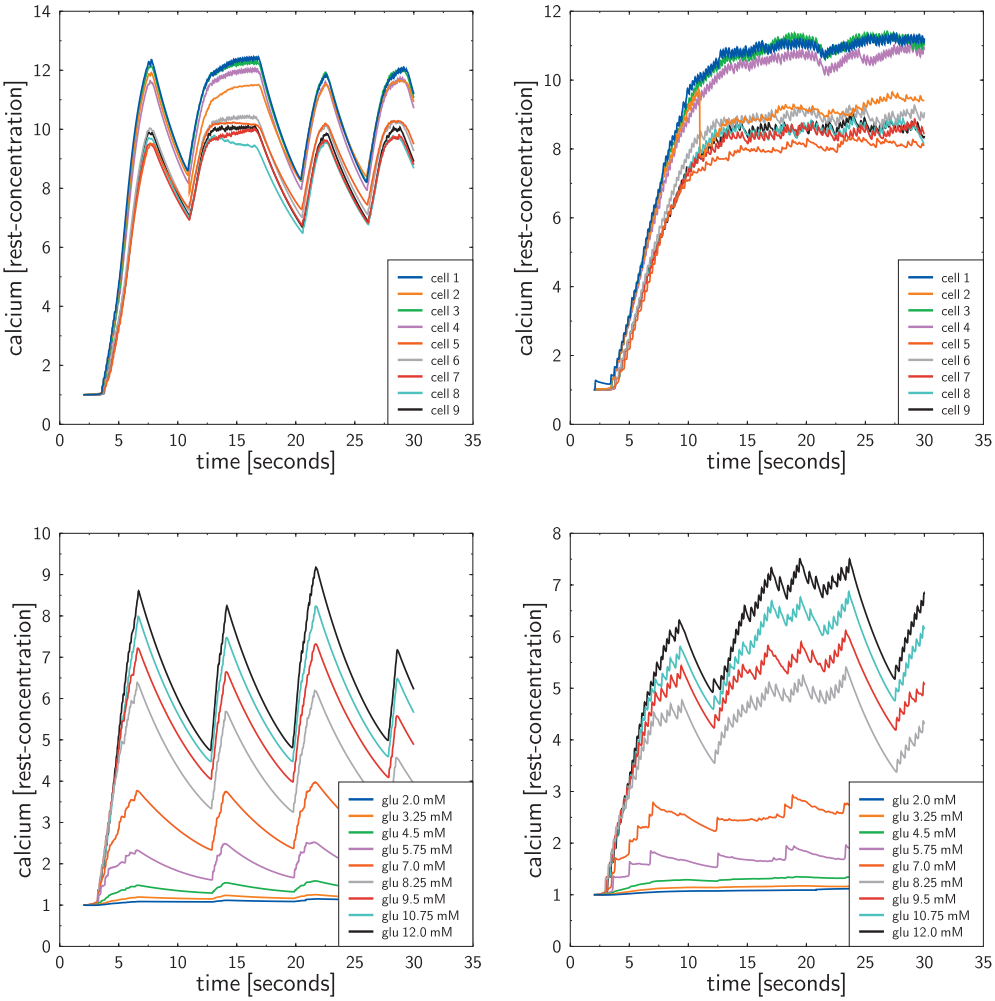

Figure 6. Impact of stochastic K-ATP channel expression. β-cell calcium levels in an islet with 27 β-cells arranged in 2D in three rows of length of nine cells. The β-cells are connected with gap-junctions (30 junctions per cell-cell contact with 5.1 pS conductance each). The expression level of K-ATP channels is randomized between 50% and 150% of the normal expression level. Gap-junction currents are delayed by 50 ms (left panels) and 500 ms (right panels). The islet is stimulated with a constant glucose level of 10 mM (upper panels) and a linear glucose gradient of 2–12 mM in the direction of the nine cells (lower panels). Even at constant glucose a grouping of β-cells in terms of calcium activity is observed (upper panels). When imposing a glucose gradient onto the islet, the transition between the active and the inactive part of the islet becomes sharp (lower panels).

are in agreement with experiment. Thus, again noise is found to strongly impact on β-cell activity in islets even though not the noise in gap-junction expression.

The situation is even more improved when assuming a delay of the gap-junctions currents. The time delay of the gap-junction Eq. (9) is formulated as a delay of the adaptation of the membrane potential. This effectively reflects a delay caused by limited ion diffusion because the membrane potential is solely built up by ions. The membrane potential itself will certainly equilibrate faster in the cell than the electrochemical gradient is set-up at the location of the gap-junction. Thus, one should be aware that this is just a phenomenological description of a spatial effect. A concise description of this phenomenon requires a spatial modeling approach including calcium buffering in organelles and explicit diffusion of ions, which is left for the future. The qualitative finding that the time delay of the adaptation of the gap-junction current to changed cell states improves the *in silico* data with respect to experiment, suggests that spatial effects may play an important role for β-cell bursting in islets of Langerhans.

MATERIALS AND METHODS

Experimental setup

Experiments were performed as described in detail (Rocheleau *et al.*, 2004). Briefly, islets were starved 1 h at 2 mM glucose, then loaded into a two channel microfluidic device. The media were delivered down two channels: one channel at 2 mM and another channel at 12 mM. NAD(P)H was imaged using two-photon microscopy with 710 nm excitation and

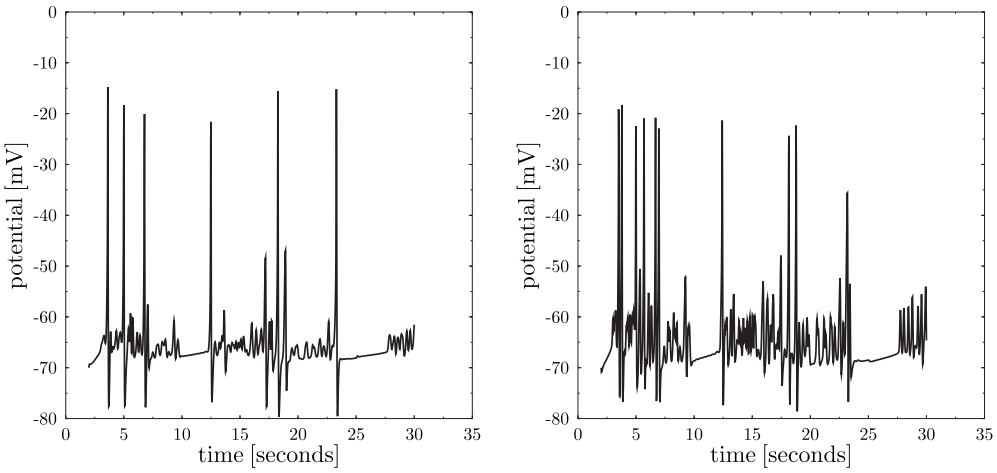

Figure 7. β-cell membrane potential of single cells in the experiment shown in Fig. 6 lower right panel. The two intermediate glucose levels 5.75 mM (left) and 7.0 mM (right) are shown.

380–550 nm detection. Calcium was imaged through staining the islet for 1–2 h with 4 μM Fluo-4 at room temperature during starvation. Fluo-4 was imaged with 488 nm excitation and 505–550 nm detection.

Simulation

Solving the set of differential equations: The set of ordinary differential equations Eqs. (1) and (3) is solved using a self-developed fourth-order Runge–Kutta algorithm. In contrast to the model without gap-junctions (Meyer-Hermann, 2007), Eq. (9) attributes to each gap-junction its own dynamics. Thus, the delay equation has to be included into the implicit solution method of the set of differential equations. Technically, this is realized by extending the cell specific properties of the β-cell-class in the C++-code by a conductance state of each of its gap-junctions.

The solver is equipped with an adaptive time step control. If a time step reduction by a factor of 2 induces an above threshold deviation of the calculation in any of the time steps, the time step is correspondingly reduced. All simulations were done in a regime of time steps in which this criterion was never met ($\Delta t = 0.00001$ s). All simulations were performed on a standard PC.

Parameter values: The values of the novel parameters added to the model in (Meyer-Hermann, 2007) are collected in Table II.

Robustness of simulations: Simulations were done in a two-dimensional *in silico* islet of 3×9 β-cells fully connected by gap-junctions. Simulations are evaluated by monitoring the electrical activity and the calcium dynamics in the central layer of the islet. The robustness of the results was tested by varying the size and the dimension of the system. On one hand a larger part of the islet with 5×9 beta-cells was used. In addition, the results were counter checked with a three-dimensional islet with $5 \times 5 \times 9$ β-cells. It turned out that the choice of the system size and dimension did not significantly impact on the results and left the conclusions untouched. The observed robustness also excludes major effects stemming from the boundary of the modeled islet. For this reason, we have chosen to present the results using the smallest system, which is easier to be presented in the graphs. In a more quantitative modeling approach small deviations stemming from the system's size and dimension would have to be considered.

The results derived for stochastic variation in transmembrane protein expression levels, where derived using a nonweighted distribution as in Eq. (15). Using a weighted distribution (such as Gaussian) mainly changes the variability range needed to reproduce the same result. In view of the missing experimental data about the variability of protein expression levels in pancreatic β-cells, we have used the simplest nonweighted distribution. The range a was varied. Smaller ranges still exhibit the grouping of β-cells that leads to the discussed sharp transition as observed in experiment. However, the calcium curves of different β-cells in the islet become less and less different with reduced variation range a.

Thus, the grouping of β-cells (in terms of activity) in the pancreatic islet turns out to be a robust feature of islets

Table II. Model parameters: the symbol, the value and the unit are given for all parameters associated with inclusion of gap-junctions into the model. All other parameter used in the model are set to the same value as in Meyer-Hermann (2007), where corresponding parameter tables are provided. The references support the value used in the model.

Variable	Value	Unit	Reference
R_{cell}	6.1	μm	Straub *et al.* (2004)
$\overline{g_{\text{gap}}}$	5.1	pS	Moreno *et al.*, (2004)
ρ_{gap}	0.385	$1/\mu\text{m}^2$	Benninger *et al.* (2008)
τ^x_{gap}	0–500	ms	Hypothetical

with variable protein expression levels. In particular, this interesting main result also persists when all ion-conducting proteins are varied with a range of $a = 0.5$ (data not shown).

If the results exhibit an unstable behavior the simulation was repeated with slightly perturbed initial conditions with a different random number generator seed value, and with a smaller time step size. In all presented cases the characteristics of the simulation results remained unchanged while the details of the time course were sensitive to the modifications.

ACKNOWLEDGMENT

M.M.H. and R.K.P.B. developed the mathematical model. M.M.H. performed the simulations. M.M.H. and R.K.P.B. wrote the article. M.M.H. and R.K.P.B. thank Jonathan V. Rocheleau and David W. Piston who developed the experimental techniques and performed the experiments (Rocheleau *et al.*, 2004) that formed the motivation and basis of the present analysis. M.M.H. thanks Michele Solimena and Jaaber Dehghani for regular and fruitful discussion. FIAS is supported by the ALTANA AG. M.M.H. is supported by the EC-NEST-project MAMOCELL. R.K.P.B. is supported by funding from the NIH under Contract Nos. K99DK85145 (to R.K.P.B.) and R01DK53434 (to D.W.P.).

REFERENCES

Allbritton, NL, Meyer, T, and Stryer, L (1992). "Range of messenger action of calcium ion and inositol 1,4,5-trisphosphate." *Science* **258**, 1812–1815.

Benninger, RK, Zhang, M, Head, WS, Satin, LS, and Piston, DW (2008). "Gap junction coupling and calcium waves in the pancreatic islet." *Biophys. J.* **95**, 5048–5061.

Chay, TR (1997). "Effects of extracellular calcium on electrical bursting and intracellular and luminal calcium oscillations in insulin secreting pancreatic β-cells." *Biophys. J.* **73**, 1673–1688.

de Vries, G (2001). "Bursting as an emergent phenomenon in coupled chaotic maps." *Phys. Rev. E* **64**, 051914.

de Vries, G, and Sherman, A (2000). "Channel sharing in pancreatic beta-cells revisited: enhancement of emergent bursting by noise." *J. Theor. Biol.* **207**, 513–530.

Gentet, LJ, Stuart, GJ, and Clements, JD (2000). "Direct measurement of specific membrane capacitance in neurons." *Biophys. J.* **79**, 314–320.

Gilon, R, Ravier, MA, Jonas, JC, and Henquin, JC (2002). "Control mechanisms of the oscillations of insulin secretion *in vitro* and *in vivo*." *Diabetes* **51**, S144–S151.

Giugliano, M, Bove, M, and Grattarola, M (2000). "Insulin release at the molecular level: metabolic-electrophysiological modeling of the pancreatic beta-cells." *IEEE Trans. Biomed. Eng.* **47**, 611–623.

Jo, J, Kang, H, Choi, MY, and Koh, D-S (2005). "How noise and coupling induce bursting action potential in pancreatic beta-cells." *Biophys. J.* **89**, 1534–1542.

Meyer-Hermann, M (2007). "The electrophysiology of the beta-cell based on single transmembrane protein characteristics." *Biophys. J.* **93**, 2952–2968.

Moreno, AP, Berthoud, VM, Pérez-Palacios, G, and Pérez-Armendariz, EM (2004). "Biophysical evidence that connexin-36 forms functional gap junction channels between pancreatic mouse beta-cells." *Am. J. Physiol. Endocrinol. Metab.* **288**, E948–E956.

Ravier, MA, Guldenagel, M, Charollais, A, Gjinovci, A, Caille, D, Sohl, G, Wollheim, CB, Willecke, K, Henquin, JC, and Meda, P (2005). "Loss of connexin 36 channels alters beta-cell coupling, islet synchronization of glucose-induced Ca^{2+} and insulin oscillations, and basal insulin release." *Diabetes* **54**, 1798–1807.

Rocheleau, JV, Remedi, MS, Granada, B, Head, WS, Koster, JC, Nichols, CG, and Piston, DW (2006). "Critical role of gap junction coupled K-ATP channel activity for regulated insulin secretion." *PLoS Biol.* **4**, e26.

Rocheleau, JV, Walker, GM, Head, WS, McGuiness, OP, and Piston, DW (2004). "Microfluidic glucose stimulation reveals limited coordination of intracellular Ca^{2+} activity oscillations in pancreatic islets." *Proc. Natl. Acad. Sci. U.S.A.* **101**, 12899–12903.

Rorsman, P, and Renstrom, E (2003). "Insulin granule dynamics in pancreatic beta cells." *Diabetologia* **46**, 1029–1045.

See supplementary material at http://dx.doi.org/10.2976/1.3354862. The movie shows the activity dynamics of 3 times 9 β-cells in a two-dimensional plane connected by gap-junctions. In the underlying simulation each cell-cell connection contains 30 gap-junctions with a conductance of 5.1 pico Siemens each. The gap-junction currents adapt to the cytosolic state of the cell with a delay of 500 milliseconds. The color codes the membrane potential of each cell from low (blue) to high (red).

Sherman, A (1996). "Contributions of modeling to understanding stimulus-secretion coupling in pancreatic beta-cells." *Am. J. Physiol.* **271**, 362–372.

Sherman, A, Rinzel, J, and Keizer, J (1988). "Emergence of organized bursting in clusters of pancreatic beta-cells by channel sharing." *Biophys. J.* **54**, 411–425.

Straub, SG, Shanmugan, G, and Sharp, GWG (2004). "Stimulation of insulin release by glucose is associated with an increase in the number of docked granules in the β-cells of rat pancreatic islets." *Diabetes* **53**, 3179–3183.

Zhang, M, Goforth, P, Bertram, R, Sherman, A, and Satin, L (2003). "The Ca^{2+} dynamics of isolated mouse beta-cells and islets: implications of mathematical models." *Biophys. J.* **84**, 2852–2870.

Zhang, Q, Galvanovskis, J, Abdulkader, F, Partridge, CJ, Goepel, SO, Eliasson, L, and Rorsman, P (2008). "Cell coupling in mouse pancreatic beta-cells measured in intact islets of Langerhans." *Philos. Trans. R. Soc. London, Ser. A* **366**, 3503–3523.